



Comparison Of Fuzzy Logic Controller (FLC) And Perturb-Observe (PO) Of Photovoltaic System

Azaza Awatef, Tlijani Hatem and Ben Younes Rached

EasyChair preprints are intended for rapid dissemination of research results and are integrated with the rest of EasyChair.

October 14, 2020

Comparison Of Fuzzy Logic Controller (FLC) And Perturb-Observe (PO) Of Photovoltaic System

AZAZA AWATEF

ENIG/Universit de Gabés/Tunisie
atoufaazaza@yahoo.com

TLIJANI HATEM

ISSAT/ Universit de Gafsa/Tunisie
hatentlijaniissat@gmail.com

BEN YOUNES RACHED

FSG/ Universit de Gafsa/Tunisie
benyounes.rached@gmail.com

Abstract—The purpose of this study is to give us a detailed comparison between the two methods of maximum power point tracking algorithm for photovoltaic systems: Perturb and Observe (PO) and fuzzy logic (FL). This occurred under different conditions of irradiation. Simulation results has indicated that the proposed fuzzy logic controller (FLC) could provides faster and stable tracking maximum power and much better behavior than (PO) methods.

Index Terms—Boost Converter, Photovoltaic (PV) System, MPPT Control, Perturb and Observe (PO), Fuzzy Logic (FL)

I. INTRODUCTION

Renewable energy technologies introduce a perfect solution such as; photovoltaic systems have received a great attention as to appear to be sustainable, limitless and environmentally friendly energy. Since global fossil sources are a limiting and polluting source and could generate the continuous growth in energy demand.

Hence, numerous studies have shown that photovoltaic (PV) modules provide nonlinear electrical characteristics which dependent on the temperature and incident irradiance [1],[3].

As a result, the I-V and P-V characteristics depend on the variation of the climatic conditions, then, the maximum power could change according to climate change. Then, it becomes necessary to use an electrical tracking system which named Maximum Power Point Tracking (MPPT). The objective of the MPPT is to ensure the efficient operation of solar PV module. In many scientific studies, there have been several MPPT techniques, such as Perturb and Observe (PO), Fuzzy Logic Control (FLC) and Sliding Mode Control (SMC). Added to, the classifications of these algorithms according to their complexity, their use and the precision of the monitoring method. Thus, the scientists have concentrated their efforts to analyze and compare the different MPPT techniques in the variations of the climatic conditions [2],[5],[6]. In this article, we have examined the performance of (PO) and (FLC) of a PV system under different irradiation conditions. In our study the PV system is composed of a PV module, a boost converter, MPPT control and a load is shown in Fig.1.

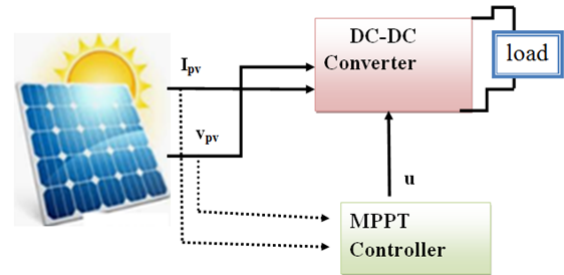


Fig. 1. PV system and load

II. MODELING OF GENERATOR PHOTOVOLTAIC :

A. Modeling of photovoltaic cell:

The equivalent circuit model of a PV cell shown in the following figure Fig.2, which is composed of a light generator source, diode, a shunt resistor expressing a leakage current, and a series resistor describing an internal resistance to the current flow [1],[3],[7].

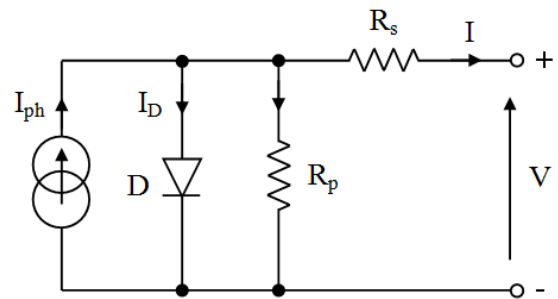


Fig. 2. Equivalent solar cells electric circuit

The equivalent model of a PV cell is using the mathematical following expression. The output current of cell can be found using kirchhoff's law in following equation:

$$I_{ph} = I + I_d + I_{Rp} \quad (1)$$

The diode current equation is described by:

$$I_d = I_s \left(e^{\frac{V+R_s I}{nV_t}} - 1 \right) \quad (2)$$

Where I_s is the reverse saturation current of the diode is dependent on the temperature can be written as:

$$I_s = \left(\frac{I_{CC}}{-1 + e^{\frac{qV_{oc}}{AKT N_s}}} \right) \left(\frac{T}{T_r} \right)^3 e^{\left(\frac{1}{T_r} - \frac{1}{T} \right) \frac{qE_g}{AK}} \quad (3)$$

The equation of the photo-current in terms of temperature and irradiation as follows:

$$I_{ph} = \frac{G}{1000} \cdot (I_{CC}(STC) + k_i \cdot (T - 298)) \quad (4)$$

The well known the output current of the cell is given by

$$I = I_{ph} - I_s \left(e^{\frac{V+R_s I}{nV_t}} - 1 \right) - \frac{(V + R_s I)}{R_p} \quad (5)$$

Where:

The parameters of PVG system are described in the following table I:

TABLE I
PARAMETER OF GPV

| |
|--|
| G : Solar radiation in (KW/m) |
| N_s : Number of series cells |
| R_s : Cell series resistance(Ω) |
| N_p : Number of shunt cells |
| R_p : Cell parallel resistance(Ω) |
| A : Ideality factor |
| I_s : Reverse diode saturation current (A) |
| I_{cc} : Short circuit current (A) |
| V : Cell output voltage (V) |
| I : Cell output current (A) |
| V_{oc} : Open circuit voltage (V) |
| q : Electric charge (1.60210-19 C) |
| n : Diode idealist factor |
| K : Boltzmann's constant (1.38110 -23 J/k) |
| K_i : Short circuit current temperature coefficient |
| T : Cell junction temperature ($^{\circ}C$) |
| T_r : Reference temperature of the PV cell ($^{\circ}C$) |
| E_g : Band gap of semi conductor used in the cell. |

B. DC/DC boost converter::

The DC/DC boost converter circuit is illustrated in the following figure Fig.3. The aim of DC/DC boost converter is to increase the voltage for source (the output voltage is greater than the input voltage) [6].

To obtain the mathematical model of the DC/DC boost converter, we may apply kirchoffs laws in each one of the circuit topologies arising as a consequence of the two switch positions:

When the switch S_w is ON, the dynamics of the circuit are:

$$\begin{cases} i_{c1}(t) = c_1 \frac{dV_{pv}(t)}{dt} = i_{pv}(t) - i_L(t) \\ i_{c2}(t) = c_2 \frac{dV_{out}(t)}{dt} = i_L(t) - i_{out}(t) \\ V_L(t) = L \frac{di_L}{dt} = V_{pv}(t) - V_{out}(t) \end{cases} \quad (6)$$

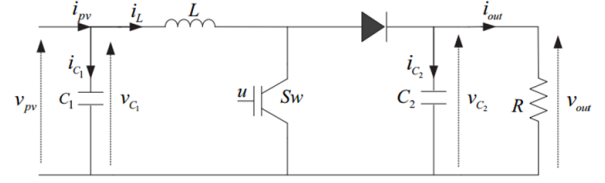


Fig. 3. DC/DC boost converter circuit

When the switch S_w is OFF, the dynamics of the circuit are:

$$\begin{cases} i_{c1}(t) = c_1 \frac{dV_{pv}(t)}{dt} = i_{pv}(t) - i_L(t) \\ i_{c2}(t) = c_2 \frac{dV_{out}(t)}{dt} = -i_{out}(t) \\ V_L(t) = L \frac{di_L}{dt} = V_{pv}(t) \end{cases} \quad (7)$$

The dynamic model final of booster converter is given by the following equation:

$$\begin{cases} i_{out}(t) = (1 - u)i_L(t) - c_2 \frac{dV_{pv}(t)}{dt} \\ i_L(t) = i_{pv}(t) - c_1 \frac{dV_{pv}(t)}{dt} \\ V_{pv}(t) = L \frac{di_L}{dt} + (1 - u)V_{out}(t) \end{cases} \quad (8)$$

So u is the duty cycle, c_1, c_2 are the capacity, L is the inductance and R is the resistive load.

C. Techniques of maximum power point tracking:

1) *Mppt based on the PO algorithm*: Due to its simplicity, the PO algorithm is the most utilized. The objective of this controller is to provoke perturbation by acting on (decrease or increase) the PWM duty cycle command and observing the output photo-voltaic generator (PVG) power reaction. If the present power $P(k)$ is greater than the last power $P(k-1)$, then the same perturbation direction. Otherwise, it is reversed [4],[8]. The PO algorithm can be explicated as follows.

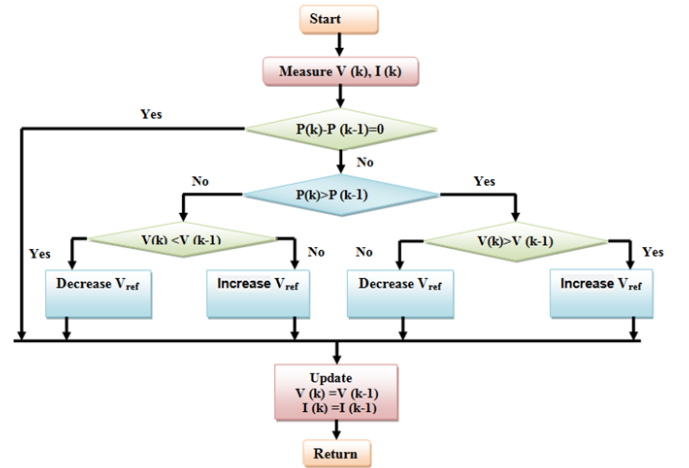


Fig. 4. Flowchart of PO algorithm

2) *Mpvt based on the FLC algorithm*: The fuzzy logic control is one of the most powerful control techniques. Indeed it has the advantage of working with imprecise entries, no need to have a precise mathematical model [2],[3],[7]. The logic controller MPPT algorithm which based on four stages: fuzzification, rule bases, fuzzy inference and defuzzification, as shown in the following figure:

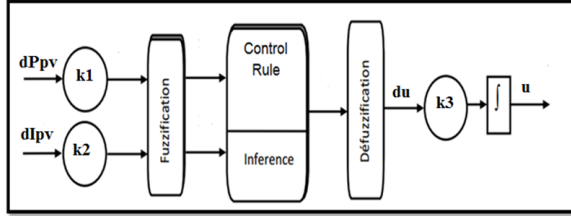


Fig. 5. Structure of FLC algorithm

* Fuzzification:

The proposed fuzzy MPPT approach has two inputs and one output. The two inputs variables of the FLC are the current variation ΔI_{pv} and the power variation ΔP_{pv} and the output variable Δu represents the variation of duty cyclic. In this work, the domain of existence is divided into seven intervals for each of the three variables ΔI_{pv} , ΔP_{pv} and the output Δu to allow good follow-up of the MPP bridge during rapid changes in lighting solar [5],[7].

* Fuzzy inference:

The following table contains the inference matrix for the controller. Input variables numerics are converted into linguistic variables to take the following seven values:

NB: Big Negative, *NM*: Medium Negative, *NS*: Small Negative, *Z*: Zero, *PS*: Small Positive, *PM*: Medium Positive, *PB*: Big Positive. The inference method chosen is MAMDANI, with an operation (Max-Min). this is to use the operator Min for the (AND), the operator Max for the (OR) [2],[7].

* Rule bases:

Table II showing fuzzy logic rules for entire system. It contains 49 fuzzy control rules. These rules are used to the control of the booster converter such as the maximum power of the solar panel. That we have reached. For example, box (7, 4) in the table represents the control rule. If dP_{pv} is *PB* and dI_{pv} is *Z* then du is *PB*. This implies that. If the operating point is away from the maximum power point (MPP) on the left side and the change in slope of the P-I curve is almost zero, then there is a large increase in the duty cycle Δu [6],[7].

* Defuzzification:

It consists in converting this time the linguistic variables into numerical variables. The process of defuzzification calculates the crisp output duty cycle Δu of the FLC. We deduce the duty cycle u by the following equation:

$$u = \Delta u(k - 1) + \Delta u \quad (9)$$

TABLE II
INFERENCE MATRIX

| dP_{pv} | dI_{pv} | | | | | | |
|-----------|-----------|-----------|-----------|-----------|-----------|-----------|-----------|
| | <i>NB</i> | <i>NM</i> | <i>NS</i> | <i>Z</i> | <i>PS</i> | <i>PM</i> | <i>PB</i> |
| <i>NB</i> | <i>PB</i> | <i>PB</i> | <i>PM</i> | <i>NB</i> | <i>NB</i> | <i>NB</i> | <i>NB</i> |
| <i>NM</i> | <i>PB</i> | <i>PM</i> | <i>PM</i> | <i>NM</i> | <i>NM</i> | <i>NM</i> | <i>NM</i> |
| <i>NS</i> | <i>PM</i> | <i>PS</i> | <i>PS</i> | <i>NS</i> | <i>NS</i> | <i>NS</i> | <i>NS</i> |
| <i>Z</i> | <i>NM</i> | <i>NM</i> | <i>NS</i> | <i>Z</i> | <i>PS</i> | <i>PS</i> | <i>PS</i> |
| <i>PS</i> | <i>NM</i> | <i>NS</i> | <i>NS</i> | <i>PS</i> | <i>PS</i> | <i>PS</i> | <i>PM</i> |
| <i>PM</i> | <i>NM</i> | <i>NM</i> | <i>NM</i> | <i>PM</i> | <i>PM</i> | <i>PM</i> | <i>PM</i> |
| <i>PB</i> | <i>NB</i> | <i>NB</i> | <i>NB</i> | <i>PB</i> | <i>PM</i> | <i>PB</i> | <i>PB</i> |

k_1 and k_2 are the inputs scaling factors, and k_3 is the defuzzification gain.

While Δu denotes the output of the fuzzy process [5],[7].

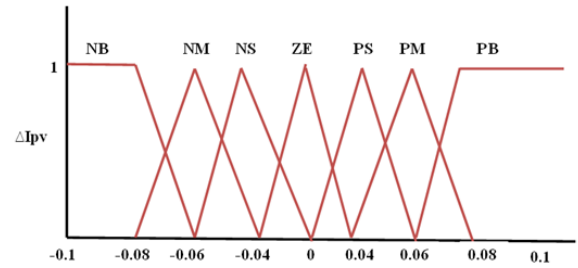


Fig. 6. Fuzzy logic control membership function for input ΔI_{pv}

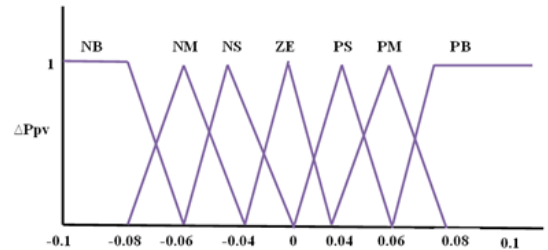


Fig. 7. Fuzzy logic control membership function for input ΔP_{pv}

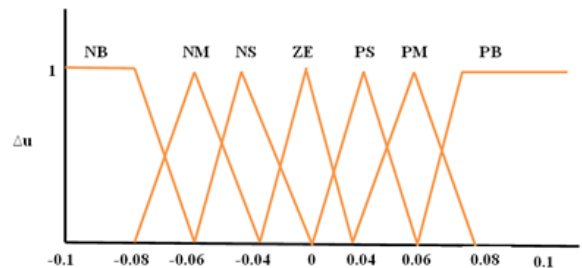


Fig. 8. Fuzzy logic control membership function for output Δu

III. SIMULATION RESULTS AND DISCUSSION:

The characteristic of PVG has a nonlinear. It is given by the Fig. 9.

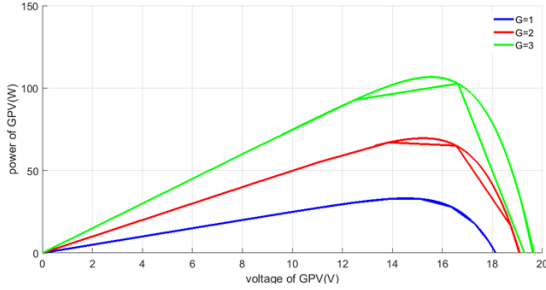


Fig. 9. P-V characteristic

The parameters of PV is given by table III.

TABLE III
PARAMETER OF GPV

| | |
|----------------------------------|--------------------------------|
| $G=1000(\text{W/m}^2)$ | $N_s=36$ |
| $R_s=0.1(\Omega)$ | $N_p=1$ |
| $K=1.38110 \cdot 23 \text{ J/k}$ | $A=1.5$ |
| $E_g=1.1$ | $I_{cc}=2.5 \text{ (A)}$ |
| $V_{oc}=21.6(\text{V})$ | $q=1.60210 \cdot 19 \text{ c}$ |

We notice that the open circuit voltage V_{oc} and the photovoltaic power increase with the high solar irradiation ($G = 1, 2, 3\text{kw m}^{-2}$) and under a constant temperature $T=25^\circ\text{C}$.

A. Influence of the solar radiation for constant temperature ($T = 25^\circ\text{C}$):

In the objective to determine the effect of realistic parameters on MPPT algorithms. The variation of irradiance levels ($G = 1, 2, 5\text{kw m}^{-2}$) to the PV array is shown in the Fig. 10 and implanted in MATLAB /Simulink environment.

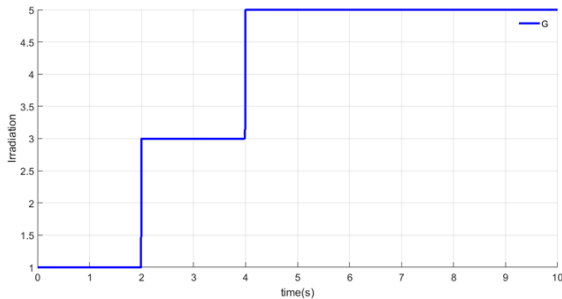


Fig. 10. Variation of irradiation as function of time

The comparison results between PO and FL algorithms are presented below Fig. 11, Fig.12, Fig. 13, Fig. 14 and Fig. 15. The Figure 11, Figure 12, Figure 13, Figure 14 and Figure 15 show respectively the variation of duty cycle " μ ",

the PV power " P_{pv} ", output current of load " I_{ch} ", output power of load " P_{ch} " and output voltage of load " V_{ch} " in tow controls: PO and Fuzzy logic

We have found that the FL controller gives good performance (reaches maximum power, faster response and absence of oscillations) than PandO which shows some oscillations at MPP level. So, from this study we could say that the MPPT controller is based on FLC theory is more performant that the classical PandO controller.

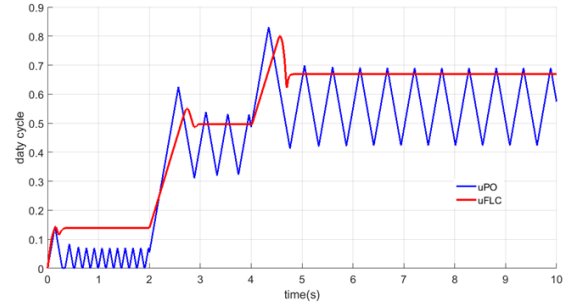


Fig. 11. The variation of duty cycle μ in tow controls: PO and Fuzzy logic

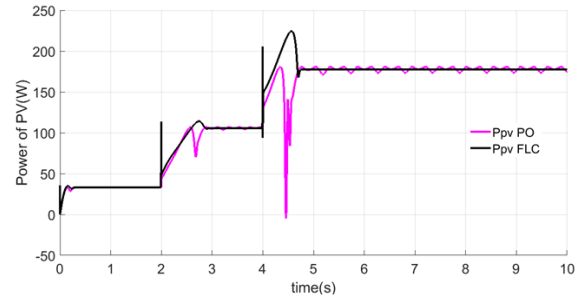


Fig. 12. The variation of PV power P_{pv} in tow controls: PO and Fuzzy logic

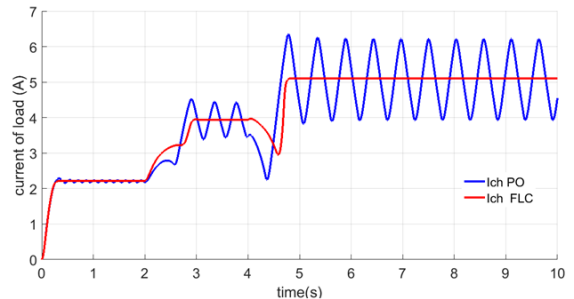


Fig. 13. The variation of output current of load I_{ch} in tow controls: PO and Fuzzy logic

The results obtained in Fig. 16, Fig. 17, Fig. 18 and Fig. 19 have shown that the boost DC-DC converter and the MPPT command that perform FLC and PO their roles correctly.

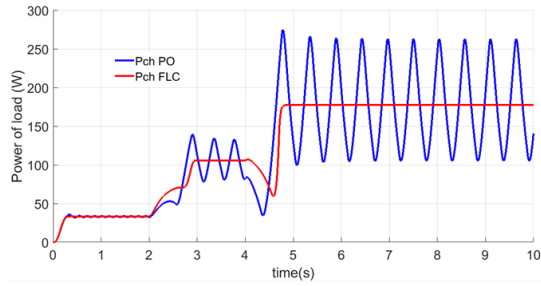


Fig. 14. The variation of output power of load P_{ch} in tow controls: PO and Fuzzy logic

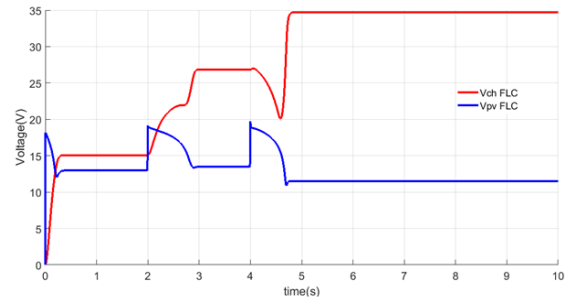


Fig. 17. The variation of output voltage of load and PV voltage for FL controller

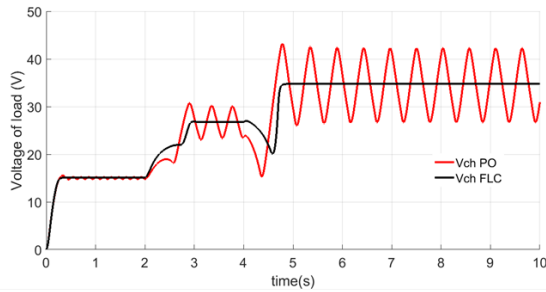


Fig. 15. The variation of output voltage of load V_{ch} in tow controls: PO and Fuzzy logic

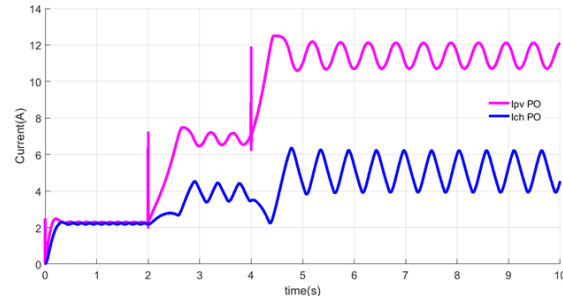


Fig. 18. The variation of output current of load and PV current for PO controller

The converter provides in optimum conditions a voltage at its output greater than that supplied by the PV generator and the current at its output lower than that supplied by the PV generator. The MPPT command which is adaptable the PV generator to the load: transfer of the maximum power supplied by the PV generator.

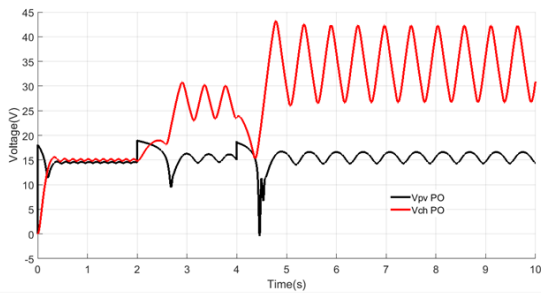


Fig. 16. The variation of output voltage of load and PV voltage for PO controller

B. Conclusion:

The two MPPT techniques which are based on respectively on the fuzzy logic and Perturb and Observe (PO) are well detailed in this work. they are modeled and evaluated according to simulations in MATLAB/ Simulink [®] environment under different irradiations conditions. Mathematical models

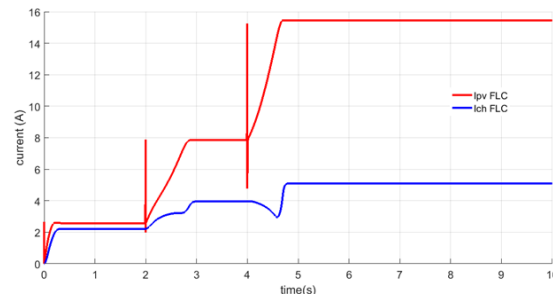


Fig. 19. The variation of output current of load and PV current for FLC controller

for different components such as (mathematical PV model and boost converter model) that have described in order to optimize the maximum power PV system MPP point.

REFERENCES

- [1] M. Ben hamed, L. Sbita, A. Flah , A. Abid, and R. Garraoui , "A real time implementation of an improved MPPT controller for photovoltaic systems," Renewable Energy and Vehicular Technology (REVET), 2012 First International Conference on, Hammamet, Tunisia, pp. 173 - 178, March 2012.
- [2] Kottas, L. Yiannis, S. Boutalis, Athanassios, and D. Karlis, " New maximum power point tracker for PV arrays using fuzzy controller in close cooperation with fuzzy cognitive networks," IEEE Transactions on Energy Conversion 21, pp.793-803, 2006.

- [3] R. Garraoui, M. Ben hamed, and L. Sbita "Comparison of MPPT Algorithms for DC-DC Boost Converters Based PV Systems using robust control technique and artificial intelligence algorithm," 12th IEEE International Conference on International Multi-Conference on Systems, Signals and Devices (SSD), March 2013.
- [4] K. Nabil, N. Moubayed, and R. Outbib, "General review and classification of different MPPT Techniques," Science Direct Journal Renewable and Sustainable Energy Reviews 68, pp.1-18, 2017.
- [5] M. Farhat, O. Barambones, and L. Sbita, "Efficiency optimization of a DSP-based standalone PV system using a stable single input fuzzy logic controller," Science Direct Journal Renewable and Sustainable Energy Reviews 49, pp.907920, 2015.
- [6] A. Messai, A. Mellit, A. Massi Pavan, A. Guessoum, and H. Mekki, "FPGA-based implementation of a fuzzy controller (MPPT) for photovoltaic module," Energy Conversion and Management 52, pp. 2695–2704, 2011.
- [7] J. Prasanth Ram, T. Sudhakar Babu, N. Rajasekar, "A comprehensive review on solar PV maximum power point tracking techniques," Renewable and Sustainable Energy Reviews 67, pp. 826847, 2017.
- [8] M. G. Villalva, J. R. Gazoli, and E. R. Filho, "Comprehensive approach to modeling and simulation of photovoltaic arrays," IEEE Trans. Power Electron., vol. 24, no. 5, pp. 11981208, May 2009.